J Vet Sci. 2022 Jan;23(1):e4
https://doi.org/10.4142/jvs.21256
pISSN 1229-845X·eISSN 1976-555X

Journal of Veterinary Science

Original Article

Molecular and Cellular Biology

Check for updates

Anti-adipogenic effect of the flavonoids through the activation of AMPK in palmitate (PA)-treated HepG2 cells

Priyanka Rajan, Premkumar Natraj, Sachithra S. Ranaweera, Lakshi A. Dayarathne, Young Jae Lee, Chang-Hoon Han*

College of Veterinary Medicine, Jeju National University, Jeju 63243, Korea

OPEN ACCESS

Received: Sep 28, 2021
Revised: Oct 20, 2021
Accepted: Nov 3, 2021
Published online: Nov 17, 2021

***Corresponding author:**
Chang-Hoon Han
College of Veterinary Medicine, Jeju National University, 102 Jejudaehak-ro, Jeju 63243, Korea.
Email: chhan@jejunu.ac.kr

ORCID iDs
Priyanka Rajan
https://orcid.org/0000-0002-0638-5808
Premkumar Natraj
https://orcid.org/0000-0003-2615-3809
Sachithra S. Ranaweera
https://orcid.org/0000-0001-9589-3240
Lakshi A. Dayarathne
https://orcid.org/0000-0001-5679-4952
Young Jae Lee
https://orcid.org/0000-0001-7892-5546
Chang-Hoon Han
https://orcid.org/0000-0002-0763-9590

ABSTRACT

Background: Flavonoids are natural polyphenols found widely in citrus fruit and peel that possess anti-adipogenic effects. On the other hand, the detailed mechanisms for the anti-adipogenic effects of flavonoids are unclear.
Objectives: The present study observed the anti-adipogenic effects of five major citrus flavonoids, including hesperidin (HES), narirutin (NAR), nobiletin (NOB), sinensetin (SIN), and tangeretin (TAN), on AMP-activated protein kinase (AMPK) activation in palmitate (PA)-treated HepG2 cells.
Methods: The intracellular lipid accumulation and triglyceride (TG) contents were quantified by Oil-red O staining and TG assay, respectively. The glucose uptake was assessed using 2-[N-(7-Nitrobenz-2-oxa-1,3-diazol-4-yl)amino]-2-deoxy-d-glucose (2-NBDG) assay. The levels of AMPK, acetyl-CoA carboxylase (ACC), and glycogen synthase kinase 3 beta (GSK3β) phosphorylation, and levels of sterol regulatory element-binding protein 2 (SREBP-2) and 3-hydroxy-3-methylglutaryl-CoA reductase (HMGCR) expression were analyzed by Western blot analysis. The potential interaction between the flavonoids and the γ-subunit of AMPK was investigated by molecular docking analysis.
Results: The flavonoid treatment reduced both intracellular lipid accumulation and TG content in PA-treated HepG2 cells significantly. In addition, the flavonoids showed increased 2-NBDG uptake in an insulin-independent manner in PA-treated HepG2 cells. The flavonoids increased the AMPK, ACC, and GSK3β phosphorylation levels and decreased the SREBP-2 and HMGCR expression levels in PA-treated HepG2 cells. Molecular docking analysis showed that the flavonoids bind to the CBS domains in the regulatory γ-subunit of AMPK with high binding affinities and could serve as potential AMPK activators.
Conclusion: The overall results suggest that the anti-adipogenic effect of flavonoids on PA-treated HepG2 cells results from the activation of AMPK by flavonoids.

Keywords: Adipogenesis; flavonoids; AMP-activated protein kinase; molecular docking; HepG2 cells

Funding

This work was supported by Korean Institute of Planning and Evaluation for Technology in Food, Agriculture and Forestry (IPET) through Innovational Food Technology Development Program, funded by Ministry of Agriculture, Food and Rural Affairs (MAFRA) (grant No. 11901303).

Authors Contributions

Conceptualization: Han CH, Rajan P; Data curation: Premkumar N; Funding acquisition: Han CH; Investigation: Rajan P, Han CH; Resources: Han CH; Software: Ranaweera SS, Dayarathne LA; Supervision: Han CH, Lee YJ; Visualization: Rajan P, Han CH; Writing-original draft: Rajan P; Writing-review & editing: Ranaweera SS, Dayarathne LA.

INTRODUCTION

AMP-activated protein kinase (AMPK) plays a vital role in controlling and regulating adipogenesis, indicating that its activation could be a promising target for anti-adipogenic strategies [1]. AMPK is a crucial energy sensor that regulates energy homeostasis by decreasing the ATP-consuming processes (fatty acid and cholesterol biosynthesis) and increasing ATP-generating processes (glucose uptake and fatty acid oxidation) [2]. AMPK activation is involved in regulating the lipid homeostasis by enhancing the phosphorylation of acetyl-CoA carboxylase (ACC), and inhibiting the sterol regulatory element-binding protein 2 (SREBP-2) and 3-hydroxy-3-methylglutaryl-CoA reductase (HMGCR), which are the key proteins responsible for fatty acid and cholesterol biosynthesis [2,3]. In addition, AMPK activation also regulates the glucose homeostasis by stimulating the non-insulin mediated glucose uptake and enhancing the phosphorylation of glycogen synthase kinase 3 beta (GSK3β), a key target in glycogen synthesis [4,5]. Therefore, AMPK is a significant target for the treatment of adipogenesis.

AMPK is a serine/threonine protein kinase that is activated by the phosphorylation at Thr172 in the α-subunit [6]. AMP binding to the γ-subunit stimulates Thr172 phosphorylation by the upstream kinases, including liver kinase B1 (LKB1) and calcium/calmodulin-dependent protein kinase kinase-β (CaMKKβ) [7]. Various *in silico* studies showed that polyphenols act as positive modulators by interacting with the γ-subunit of AMPK, similar to AMP [8,9]. Accordingly, a direct activator of AMPK that would mimic the mechanism of AMP might be a suitable therapeutic strategy against adipogenesis.

Increasing attention has focused on natural plant flavonoids to develop novel anti-adipogenic drugs with high efficacy and few side effects. Flavonoids are natural polyphenolic compounds present in citrus fruit and peel at high concentrations [10]. A recent study showed that immature citrus fruits are rich in five flavonoids, including 2 flavone glycosides (hesperidin and narirutin) and three polymethoxylated flavones (nobiletin, sinensetin, and tangeretin) (**Fig. 1**) [10]. These flavonoids exhibit a wide range of promising pharmaceutical effects, including anti-adipogenic effects [11-13]. On the other hand, the detailed mechanisms for the anti-adipogenic

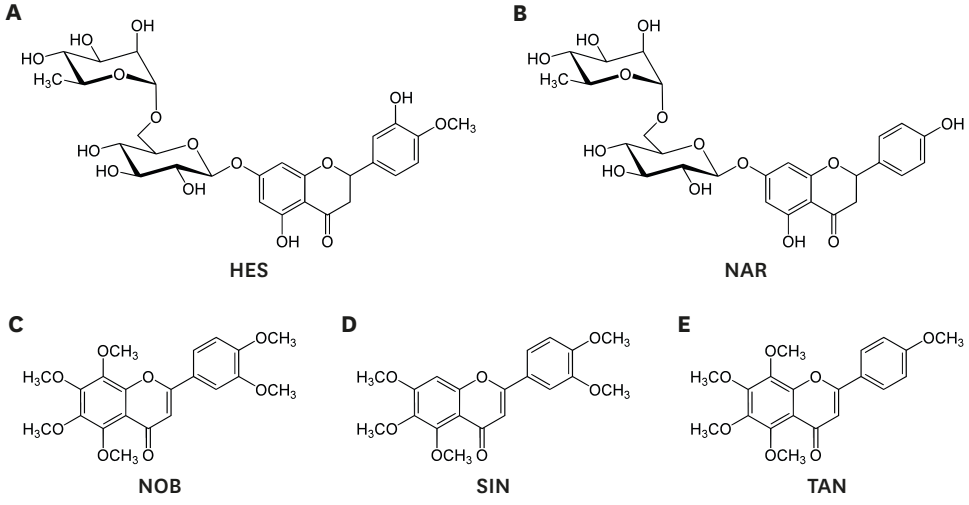

Fig. 1. Chemical structure of HES (A), NAR (B), NOB (C), SIN (D), and TAN (E).
HES, hesperidin; NAR, narirutin; NOB, nobiletin; SIN, sinensetin; TAN, tangeretin.

effects of these flavonoids are unclear. In this context, an adipogenic model was established using palmitate (PA)-treated HepG2 cells [14] to explore the anti-adipogenic effects of the five major citrus flavonoids and the molecular mechanism underlying their effects.

The present study hypothesized that the five major citrus flavonoids possess anti-adipogenic effects by activating the AMPK pathway in PA-treated HepG2 cells. For this, the effects of the flavonoids on lipid accumulation, triglyceride (TG) content, and glucose uptake were evaluated. AMPK and its downstream substrates involved in lipid metabolism were analyzed to determine the molecular mechanisms underlying their effects. *In silico* analysis was performed to investigate the AMPK-activating capacity of the flavonoids and assess the primary mechanism of action. These results might offer a valuable clue for elucidating the mechanism of the anti-adipogenic effects of the flavonoids through AMPK activation.

MATERIALS AND METHODS

Cell culture and treatment

Human hepatoma HepG2 cells were purchased from the Korean Cell Line Bank (KCLB, Korea) and cultured in Dulbecco's modified Eagle's medium (DMEM) supplemented with 10% fetal bovine serum (FBS), 1% penicillin, and streptomycin (Gibco, USA) in a humidified atmosphere under 5% CO_2 at 37°C. HepG2 cells were seeded in 96-well plates. After reaching confluence, the cells were serum-starved overnight and exposed to 0.4 mM PA (Sigma-Aldrich, USA), in the presence or absence of 5 μM simvastatin (Sigma-Aldrich), 2 mM metformin (Sigma-Aldrich), 50 μM of hesperidin (LKT Laboratories, USA), narirutin (Sigma-Aldrich), nobiletin (Sigma-Aldrich), sinensetin (Sigma-Aldrich), or tangeretin (Sigma-Aldrich) for 24 h. The cells treated with simvastatin or metformin were used as the positive control.

Preparation of PA

PA-bovine serum albumin (BSA) conjugate was made by soaping of PA with sodium hydroxide (NaOH) and blending with BSA (Sigma-Aldrich), as described previously [15]. Briefly, palmitate (25 mM) was diluted in NaOH (50 mM) at 70°C for 30 min and mixed with 10% BSA (Sigma-Aldrich) at 55°C for 15 min as a 5 mM reserving solution. The reserving solution was diluted in serum-free DMEM to obtain a 0.4 mM palmitate solution.

Cell viability assay

The cell viability was assessed by a 3-(4,5-dimethylthiazol-2-yl)-2,5 diphenyltetrazolium bromide (MTT) assay using an EZ-cytox assay kit (Dogen Bio, Korea). HepG2 cells were seeded into 96-well plates at 1×10^5 cells per well. The cells were treated with varying concentrations of PA, hesperidin (HES), narirutin (NAR), nobiletin (NOB), sinensetin (SIN), and tangeretin (TAN) for 24 h. After removing the culture media, fresh media containing 10% EZ-cytox in DMEM was added to each well. The cells were maintained at 37°C and 5% CO_2 for 3 h to allow the formation of formazan. After 3 h incubation, absorbance was measured at 450 nm using an enzyme-linked immunosorbent assay microplate reader (TECAN, Austria).

Oil Red O staining

Intracellular lipid accumulation was determined by Oil Red O staining using a previously reported method with slight modifications [16]. HepG2 cells were plated in a 96-well plate at a density of 1×10^5 cells/well. After treatment, the HepG2 cells were rinsed with phosphate-buffered saline (PBS) and fixed with 10% formaldehyde for 1 h. The cells were

rinsed with 60% isopropanol and stained with Oil Red O (Sigma-Aldrich) for 30 min at room temperature. The cells were rinsed with sterile water four–five times to remove excess staining solution. IncuCyte ZOOM (Essen BioScience, USA) was used to capture and analyze the images at 20× magnification.

TG assay

The cellular triglyceride contents were evaluated using a commercially available triglyceride colorimetric assay kit (BioAssay Systems, USA). After treatment, the cells were rinsed with PBS and collected in a cell lysis buffer containing 5% Triton X-100. The cells were homogenized, followed by centrifugation at 3,000 × *g* for 5 min. The triglyceride content of the supernatant was examined according to the manufacturer's instructions. The protein concentration was quantified using a Bio-Rad DC protein assay (Bio-Rad Laboratories, USA). The triglycerides contents were normalized to the protein concentration, as determined by BSA as the calibration standard.

Two-[N-(7-Nitrobenz-2-oxa-1,3-diazol-4-yl)amino]-2-deoxy-d-glucose (2-NBDG) uptake assay

The glucose uptake in HepG2 cells was assessed using a 2-NBDG assay. Briefly, HepG2 cells were plated in a 96-well plate at a density of 1×10^5 cells/well. After the treatments, the cells were exposed to 40 μM 2-NBDG (Carlsbad, USA) in the presence or absence of insulin (100 nM) for 30 min at 37°C. The cells were rinsed with PBS, and fluorescent images were captured using IncuCyte ZOOM (Essen BioScience, USA) at 20× magnification. Fluorescence analysis was carried out using IncuCyte ZOOM Fluorescent Processing software.

Preparation of cell lysates and Western blot analysis

HepG2 cells were seeded in a 24-well plate at a density of 5×10^4 cells/well. After the treatments, the cells were rinsed with PBS and lysed with ice-cold RIPA buffer (20 mM Tris-HCl pH 7.5, 150 mM NaCl, 1 mM EGTA, 1 mM Na_2 EDTA, 1% NP-40, 1% sodium deoxycholate, 2.5 mM sodium pyrophosphate, 1 mM $NaVO_4$, and 1 μg/mL leupeptin) containing protease inhibitor. The whole-cell lysate was centrifuged at 12,000 rpm for 10 min, and the supernatants were collected and assayed for the protein concentration using the Bradford assay kit (Bio-Rad Laboratories). For Western blotting, an equal amount of protein was separated by 10% sodium dodecyl sulphate-polyacrylamide gel electrophoresis and transferred electrophoretically to a nitrocellulose membrane. The membranes were blocked with 5% non-fat dry milk in Tris-buffered saline with 0.1% Tween 20. The membranes were incubated with the primary antibodies for AMPK (Cell Signaling Technology, USA), p-AMPK (Thr172) (Cell Signaling Technology), ACC (Cell Signaling Technology), p-ACC (Ser79) (Cell Signaling Technology), GSK3β (Cell Signaling Technology), p-GSK3β (Ser9) (Cell Signaling Technology), β-actin (Thermo Fisher, USA), SREBP-2 (Thermo Fisher), and HMGCR (Thermo Fisher), followed by incubation with the HRP-conjugated secondary antibodies. Immunoreactive bands were analyzed using a Chemi-luminescence Bioimaging Instrument (NeoScience, Korea).

Molecular docking

The crystal structure of AMPK in the complexes with AMP (PDB ID; 2V8Q) was obtained from Protein Data Bank (PDB). The sitemap tool (Schrodinger Software, Germany) was used to identify the 4 cystathionine-β-synthase (CBS) domains (CBS1, CBS2, CBS3, and CBS4) in the γ-subunit of AMPK. All AMP molecules in the γ-subunit of AMPK were removed for docking flavonoids. The 3D structures of AMP and the flavonoids (HES, NAR, NOB, SIN, and TAN) were obtained from the PubChem database (https://pubchem.ncbi.nlm.nih.gov/) and

minimized energetically using PyRx software (Python Prescription 0.8; The Scripps Research Institute, USA). The grid box used for focused docking was set to 26×44×46 Å to ensure the structure of the γ-subunit of AMPK. The docking experiments were carried out using the AutoDock Vina module (Molecular Graphics Lab, The Scripps Research Institute). Based on binding energy, the best-docked pose was selected, and the 3D images were produced using the PyMOL (The PyMOL Molecular Graphics System, Ver.2.5.0; Schrodinger, LLC, USA). Docked complex of AMPK was optimized further, validated, and explored using Discovery Studio visualizer (Ver.21.1.0.20298). The hydrogen bond and hydrophobic interactions between the receptor and ligand were analyzed using the Ligplot program [17].

Statistical analysis

The data are expressed as the means ± SE of 3 independent experiments and analyzed statistically using IBM SPSS Statistics (Ver.17.0; IBM Corp., USA). The statistical differences among the groups were analyzed by one-way analysis of variance (ANOVA) followed by a Tukey's test. The following were considered significant differences from the PA-treated control group: $p < 0.05$, $p < 0.005$, and $p < 0.0005$.

RESULTS

Cell viability

A MTT assay was performed to evaluate the cytotoxicities of HES, NAR, NOB, SIN, and TAN on HepG2 cells (**Fig. 2**). HepG2 cells were treated with different concentrations of PA, HES, NAR, NOB, SIN, or TAN for 24 h to examine the cell viability. PA did not exhibit any cytotoxicity up to 500 μM (**Fig. 2A**). The flavonoids did not have any cytotoxic effects at concentrations up to 100 μM (**Fig. 2B-F**). Accordingly, 400 μM of PA and 50 μM of the flavonoids were used in the following experiments.

Intracellular lipid accumulation and TG content

Oil Red O staining and a TG assay were carried out to assess the effect of HES, NAR, NOB, SIN, and TAN on intracellular lipid accumulation and TG content in HepG2 cells (**Fig. 3**). HepG2 cells treated with PA increased ($p < 0.0005$) lipid accumulation and TG content significantly compared to the untreated control cells. The cells treated with SIM (positive control) showed significantly lower ($p < 0.005$) lipid accumulation and TG content than the PA-treated control cells. In addition, the cells treated with HES, NAR, NOB, SIN, or TAN showed significantly lower ($p < 0.005$) lipid accumulation and TG contents than the PA-treated control cells (**Fig. 3A-C**). Overall, the results suggest that HES, NAR, NOB, SIN, and TAN markedly reduced the lipid accumulation and TG content in PA-treated HepG2 cells.

Glucose uptake

A 2-NBDG uptake assay was carried out to examine the effects of HES, NAR, NOB, SIN, and TAN on the glucose uptake in PA-treated HepG2 cells (**Fig. 4**). The HepG2 cells treated with PA showed lower glucose uptake compared to the untreated control cells. On the other hand, the cells treated with MET showed significantly higher ($p < 0.005$) glucose uptake. In particular, the cells treated with HES, NAR, NOB, SIN, or TAN showed significantly enhanced ($p < 0.005$) glucose uptake compared to the PA-treated control cells, regardless of insulin stimulation (**Fig. 4A and B**). These results suggest that the HES, NAR, NOB, SIN, and TAN treatment improved the glucose uptake in an insulin-independent manner in PA-treated HepG2 cells.

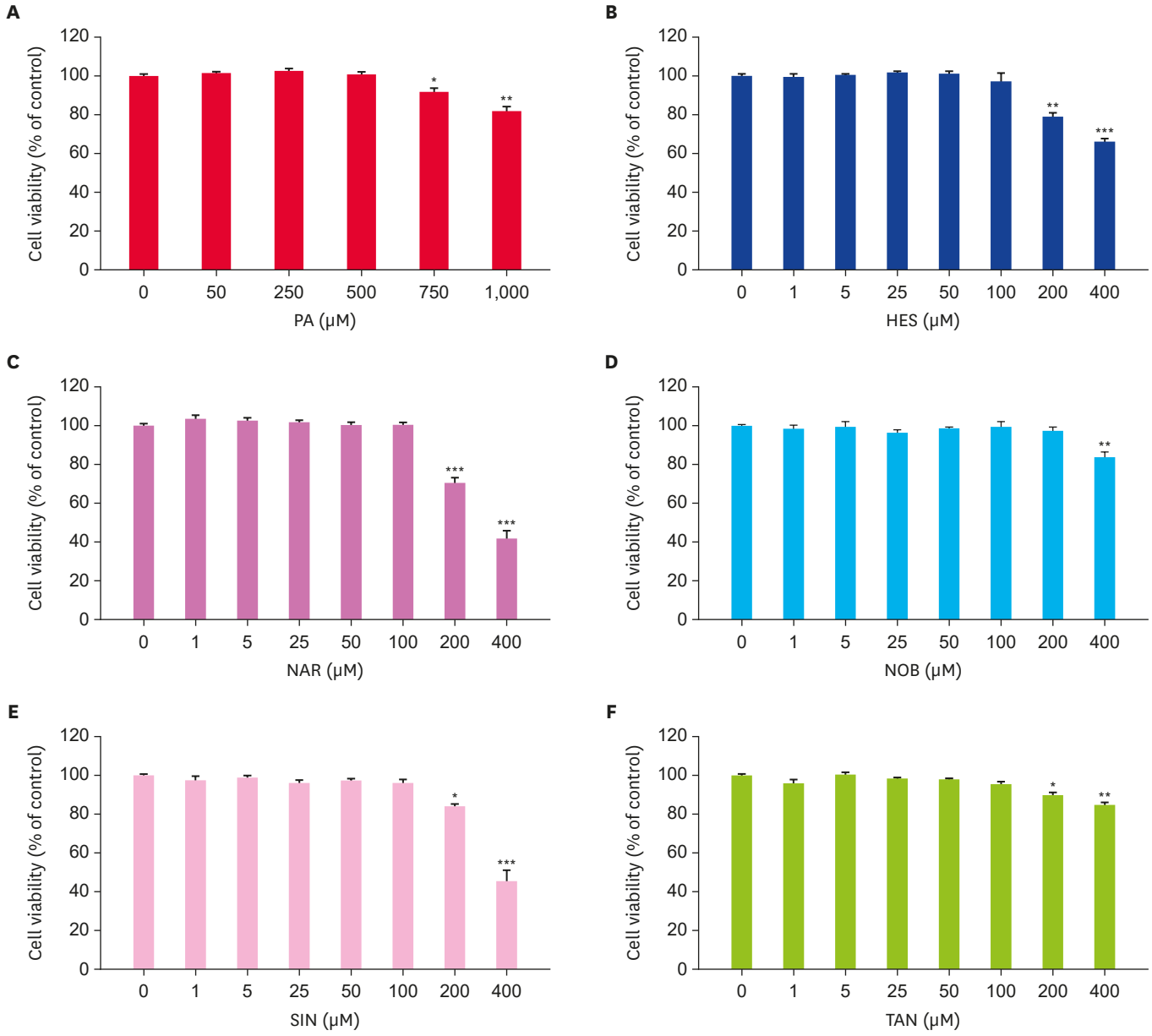

Fig. 2. Effect of the flavonoids on the HepG2 cell viability. The cells were incubated with indicated concentrations of (A) PA, (B) HES, (C) NAR, (D) NOB, (E) SIN, or (F) TAN for 24 h. A MTT assay was performed to assess the cell viability (A-F). Data are represented as the mean ± SE.
PA, palmitate; HES, hesperidin; NAR, narirutin; NOB, nobiletin; SIN, sinensetin; TAN, tangeretin; MTT, 3-(4,5-dimethylthiazol-2-yl)-2,5-diphenyltetrazolium bromide.
$^{*}p < 0.05$, $^{**}p < 0.005$, $^{***}p < 0.0005$ compared to the control.

AMPK signaling pathway

The effects of HES, NAR, NOB, SIN, and TAN on the phosphorylation of AMPK (Thr172) and ACC (Ser79) and the levels of SREBP2 and HMGCR expression in PA-treated HepG2 cells were analyzed by Western blot (**Fig. 5**). The results showed that the treatment with PA significantly decreased ($p < 0.05$) the AMPK (Thr172) and ACC (Ser79) phosphorylation levels and increased ($p < 0.005$) the SREBP2 and HMGCR expression levels. By contrast, the treatment with HES, NAR, NOB, SIN, and TAN significantly increased ($p < 0.05$) the AMPK (Thr172) and ACC (Ser79) phosphorylation levels in PA-treated HepG2 cells and reduced ($p < 0.005$) the SREBP2 and HMGCR expression levels significantly (**Fig. 5A-D**). These results

https://doi.org/10.4142/jvs.21256

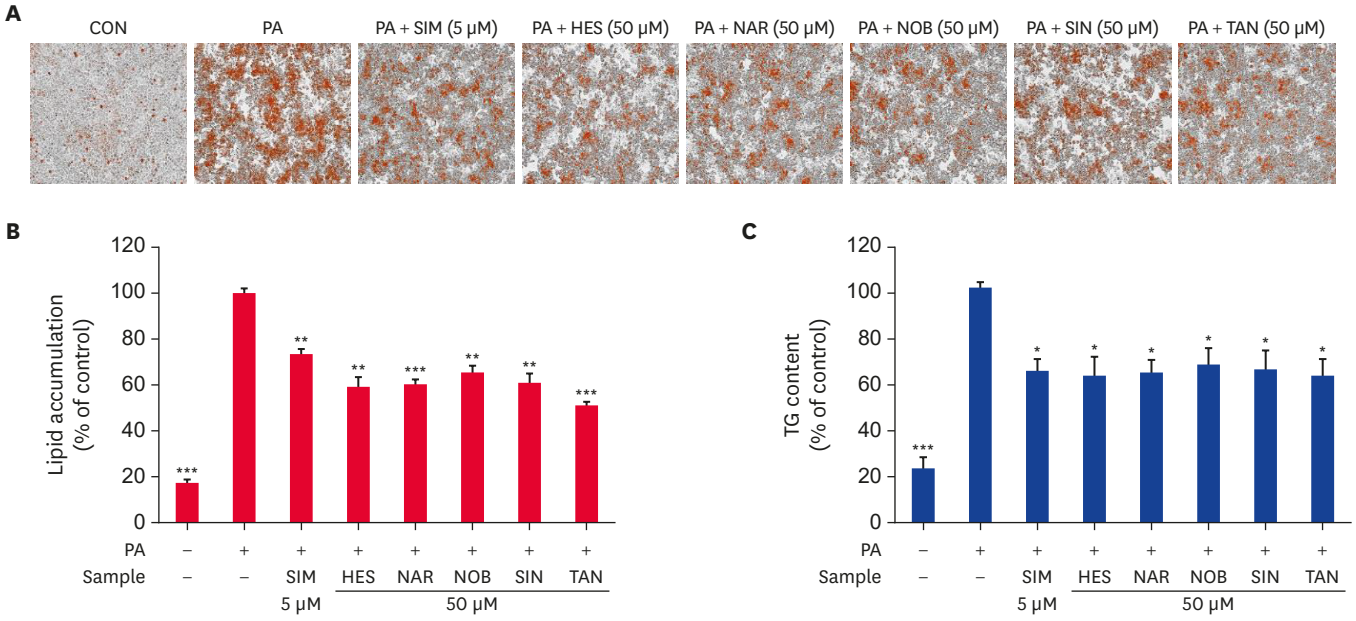

Fig. 3. Effect of the flavonoids on intracellular lipid accumulation and TG content in PA-treated HepG2 cells. HepG2 cells were serum-starved overnight and incubated in a serum-deprived medium containing PA with or without 50 μM flavonoids for 24 h. The lipid accumulation of HepG2 cells was observed by Oil Red O staining and analyzed using IncuCyte ZOOM fluorescence processing software at 20× magnification (A). Quantitative measurement of lipid accumulation using IncuCyte ZOOM fluorescence-processing software (B). Relative intracellular TG content was detected using the TG assay kit (C). Data are presented as the mean ± SE.
TG, triglyceride; CON, control; PA, palmitate; SIM, simvastatin; HES, hesperidin; NAR, narirutin; NOB, nobiletin; SIN, sinensetin; TAN, tangeretin.
$^{*}p < 0.05$, $^{**}p < 0.005$, $^{***}p < 0.0005$ compared to the PA-treated control.

suggest that the flavonoids activate the AMPK pathway and have an anti-adipogenic effect on PA-treated HepG2 cells.

Phosphorylation of GSK3β

The effects of HES, NAR, NOB, SIN, and TAN on the phosphorylation of GSK3β in PA-treated HepG2 cells were observed by Western blot analysis (**Fig. 6**). Based on densitometry analysis, the HepG2 cells treated with PA showed significantly lower ($p < 0.05$) phosphorylation levels of GSK3β than the untreated control cells. On the other hand, the MET treatment significantly increased ($p < 0.05$) the level of GSK3β phosphorylation compared to the PA-treated control cells. In addition, the treatment with HES, NAR, NOB, SIN, or TAN increased ($p < 0.05$) the level of GSK3β phosphorylation remarkably compared to PA-treated control cells (**Fig. 6**). The results show that the flavonoids increase the level of GSK3β phosphorylation in the PA-treated HepG2 cells.

Molecular docking analysis

Molecular docking analysis was performed to determine the potential interactions between the flavonoids (HES and NAR) and the γ-subunit of AMPK (**Fig. 7**). **Fig. 7A and B** show the crystallographic and the domain structures of the α, β, and γ subunits of AMPK, respectively. The γ-subunit contains 4 tandem repeats of CBS domains. Among the four CBS domains, only 3 (CBS1, CBS3, and CBS4) domains can bind to its true modulators, adenine nucleotides, including AMP, ADP, and ATP. As shown in **Table 1**, the flavonoids (HES, NAR, NOB, SIN, and TAN) bind to the binding sites (CBS1, CBS3, and CBS4) with high binding affinities that are close to the affinity of true modulator AMP. In particular, both HES and NAR showed higher binding affinities than the true modulator, AMP, at all three CBS domains. In particular, both HES and NAR form more hydrogen bonds or hydrophobic interactions than AMP (**Table 1**).

https://doi.org/10.4142/jvs.21256

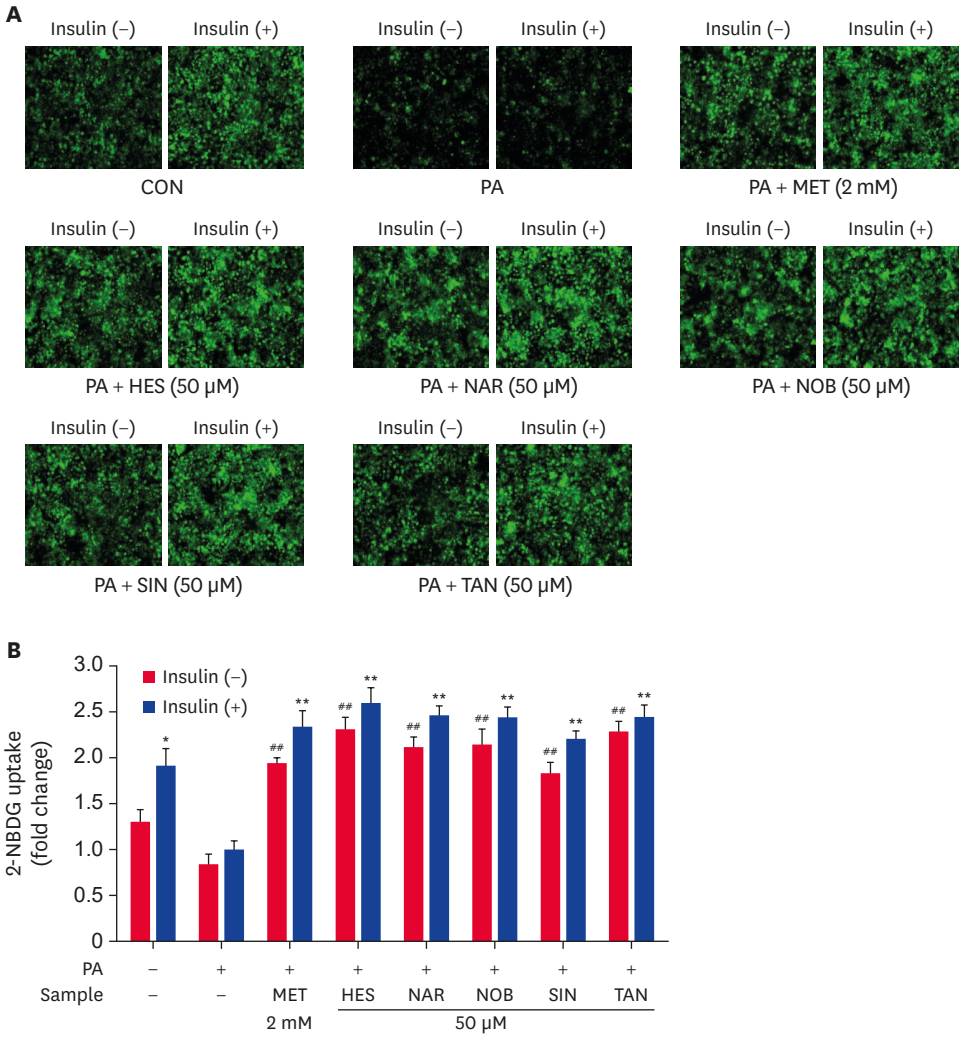

Fig. 4. Effect of the flavonoids on glucose uptake in PA-treated HepG2 cells. The glucose uptake assay was carried out using the fluorescent D-glucose analog 2-NBDG. HepG2 cells were serum-starved overnight and incubated in a serum-deprived medium containing PA with or without 50 μM flavonoids for 24 h. followed by incubation with 40 μM 2-NBDG glucose in the presence or absence of 100 nM insulin for 30 min. The cells were rinsed with PBS, and the fluorescence images were captured by IncuCyte ZOOM at 20× magnification (A). The total fluorescence intensities were calculated using IncuCyte ZOOM fluorescence processing software (B). The data are presented as the mean ± SE.
2-NBDG, 2-[N-(7-Nitrobenz-2-oxa-1,3-diazol-4-yl)amino]-2-deoxy-d-glucose; CON, control; PA, palmitate; MET, metformin; HES, hesperidin; NAR, narirutin; NOB, nobiletin; SIN, sinensetin; TAN, tangeretin.
$^{*}p < 0.05$, $^{**}p < 0.005$ compared to the insulin-stimulated PA-treated control and $^{\#}p < 0.05$, $^{\#\#}p < 0.005$ compared to the non-insulin-stimulated PA-treated control.

The overall results show that the flavonoids bind to the regulatory γ-subunit of AMPK with high binding affinities, suggesting that the flavonoids can serve as positive modulators for AMPK activation.

DISCUSSION

The present study evaluated the anti-adipogenic effect of citrus flavonoids associated with AMPK activation in PA-treated HepG2 cells. The flavonoids reduced the intracellular

https://doi.org/10.4142/jvs.21256

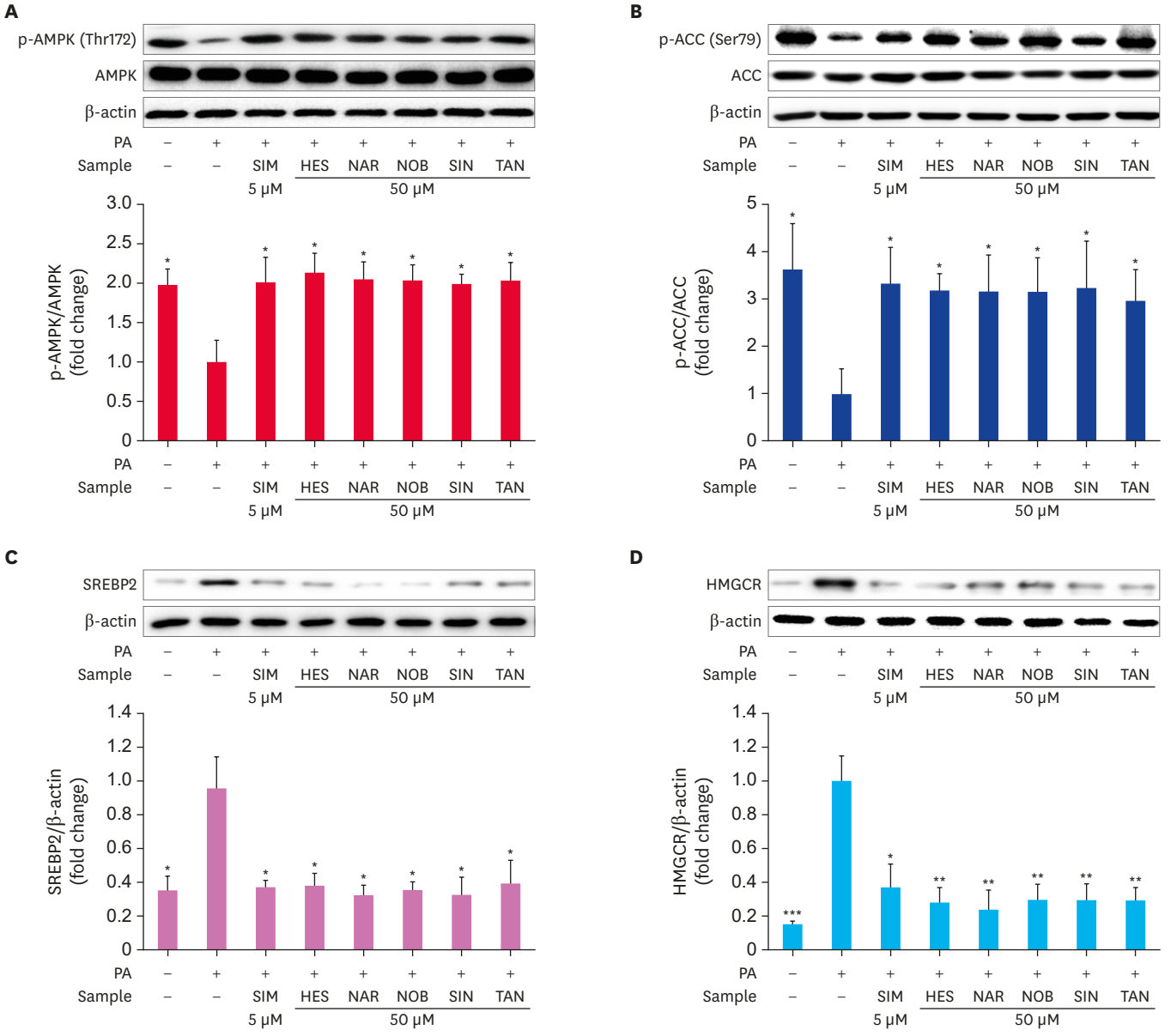

Fig. 5. Effects of the flavonoids on the AMPK and ACC phosphorylation levels and the SREBP-2 and HMGCR expression levels in PA-treated HepG2 cells. HepG2 cells were serum-starved overnight and incubated in a serum-deprived medium containing PA with or without flavonoids for 24 hrs. p-AMPK and p-ACC and the expression of SREBP-2 and HMGCR were determined by Western blotting. Representative immunoblots of p-AMPK (A), p-ACC (B), SREBP-2 (C), and HMGCR (D). The relative protein levels were measured using densitometry analysis. Data are represented as the mean ± SE.
AMPK, AMP-activated protein kinase; ACC, acetyl-CoA carboxylase; SREBP-2, sterol regulatory element-binding protein 2; HMGCR, 3-hydroxy-3-methylglutaryl-CoA reductase; PA, palmitate; SIM, simvastatin; HES, hesperidin; NAR, narirutin; NOB, nobiletin; SIN, sinensetin; TAN, tangeretin.
$^{*}p < 0.05$, $^{**}p < 0.005$, $^{***}p < 0.0005$ compared to PA-treated control.

lipid accumulation and TG content significantly, and enhanced the glucose uptake in an insulin-independent manner in PA-treated HepG2 cells. In addition, the flavonoid-mediated AMPK activation increased the ACC phosphorylation level and decreased the SREBP-2 and HMGCR expression levels, which are crucial for lipogenesis and cholesterol biosynthesis. Furthermore, the flavonoids increased GSK3β phosphorylation levels, which is a critical enzyme in glycogen synthesis. Molecular docking analysis showed that the flavonoids bind to the CBS domain in the regulatory γ-subunit with high binding affinities, suggesting that the flavonoids could be positive modulators of AMPK activation.

https://doi.org/10.4142/jvs.21256

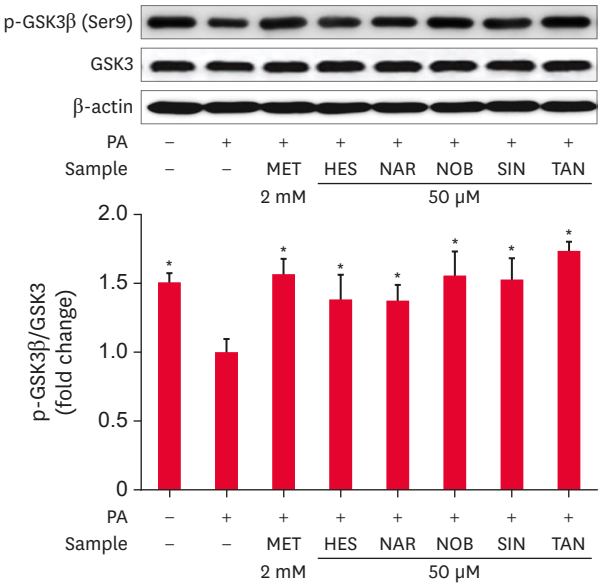

Fig. 6. Effects of the flavonoids on the GSK3β phosphorylation level in PA-treated HepG2 cells. HepG2 cells were serum-starved overnight and incubated in a serum-deprived medium containing PA with or without 50 μM flavonoids for 24 h. p-GSK3β was determined by Western blotting. The data are represented as the mean ± SE. GSK3β, glycogen synthase kinase 3 β; PA, palmitate; MET, metformin; HES, hesperidin; NAR, narirutin; NOB, nobiletin; SIN, sinensetin; TAN, tangeretin.
*$p < 0.05$ compared to PA-treated control.

The present study showed that the flavonoids suppressed the intracellular lipid accumulation and TG content induced by PA in HepG2 cells. A previous study reported that a mixture of

Table 1. Binding energy of AMP and flavonoids at three domains that were identified in the γ-subunit of AMPK

Molecule	Description	Binding site of γ-subunit of AMPK		
		CBS1	CBS3	CBS4
AMP	Binding energy (kcal/mol)	−7.8	−7.4	−8.1
	Hydrogen bonds	D89, T88, K148, R151, H150, T86	A294, S241, D244, R268, R298, K169, H297, R69	N202, S225, S313, H297, S315, H150
	Hydrophobic interactions	M84, I149, I87	L276, I239, V296, F243	I203, V224, I311, T199, K148
HES	Binding energy (kcal/mol)	−9.1	−9	−8.8
	Hydrogen bonds	P127, K126, R117, M84, R151, R223	K169, S241, R69, E295, R298, E273	L144, K148, I149, H168, S315, R223, S225
	Hydrophobic interactions	W116, L128, V129, I149, T86, I87, D89, T120, L121, K148, T88, H150, K242, R69	F243, H270, V296, Y271, F272, I239, L276, V300, G274	I145, D316, Q319, S313, T199, V224, R298, H297, A226, I311
NAR	Binding energy (kcal/mol)	−8.3	−9	−9.3
	Hydrogen bonds	H150, R151, V129, K148, T86, V220, P127	E273, E295, K169, S241	K148, I149, L144, H168, S315, R223, R298, A226
	Hydrophobic interactions	I149, T88, M84, P153, L128, N92, R223, D89, W116, L121, Y120	Y271, H270, F272, V296, G274, L276, I239, F243, R69, R298	I145, T199, Q319, D316, V224, S313, S225, I311
NOB	Binding energy (kcal/mol)	−7.5	−7	−7.7
	Hydrogen bonds	M84, H150, K242	R298	T199, S225
	Hydrophobic interactions	R117, V182, K126, D89, W116, L121, L128, G83, T88, T86, I149, R223	L276, I239, V296, F272, S241, H270, R69, F243	A204, A226, I203, V224, I311, R298, N202, S315, K148, H150, I145, I149
SIN	Binding energy (kcal/mol)	−7.6	−6.9	−7.8
	Hydrogen bonds	M84, H150	R298	S225
	Hydrophobic interactions	V82, G83, K126, L121, L128, R117, I149, W116, D89, T86, T88, K242, R223	L276, I239, F272, V296, H270, S241, F243, R69	A204, R298, A226, I311, I203, V224, N202, T199, S313, Q319, D316, K148, S315, I145
TAN	Binding energy (kcal/mol)	−6.9	−7.1	−7.3
	Hydrogen bonds	M84	R298	S225, T199
	Hydrophobic interactions	V82, R117, G83, W116, K126, L128, L121, T86, D89, I149, T88, H150, R223	I239, F272, L276, S241, H270, V296, R69, F243	I311, V224, A226, R298, S315, K148, I145

AMPK, AMP-activated protein kinase; CBS, cystathionine-β-synthase; HES, hesperidin; NAR, narirutin; NOB, nobiletin; SIN, sinensetin; TAN, tangeretin.

https://doi.org/10.4142/jvs.21256

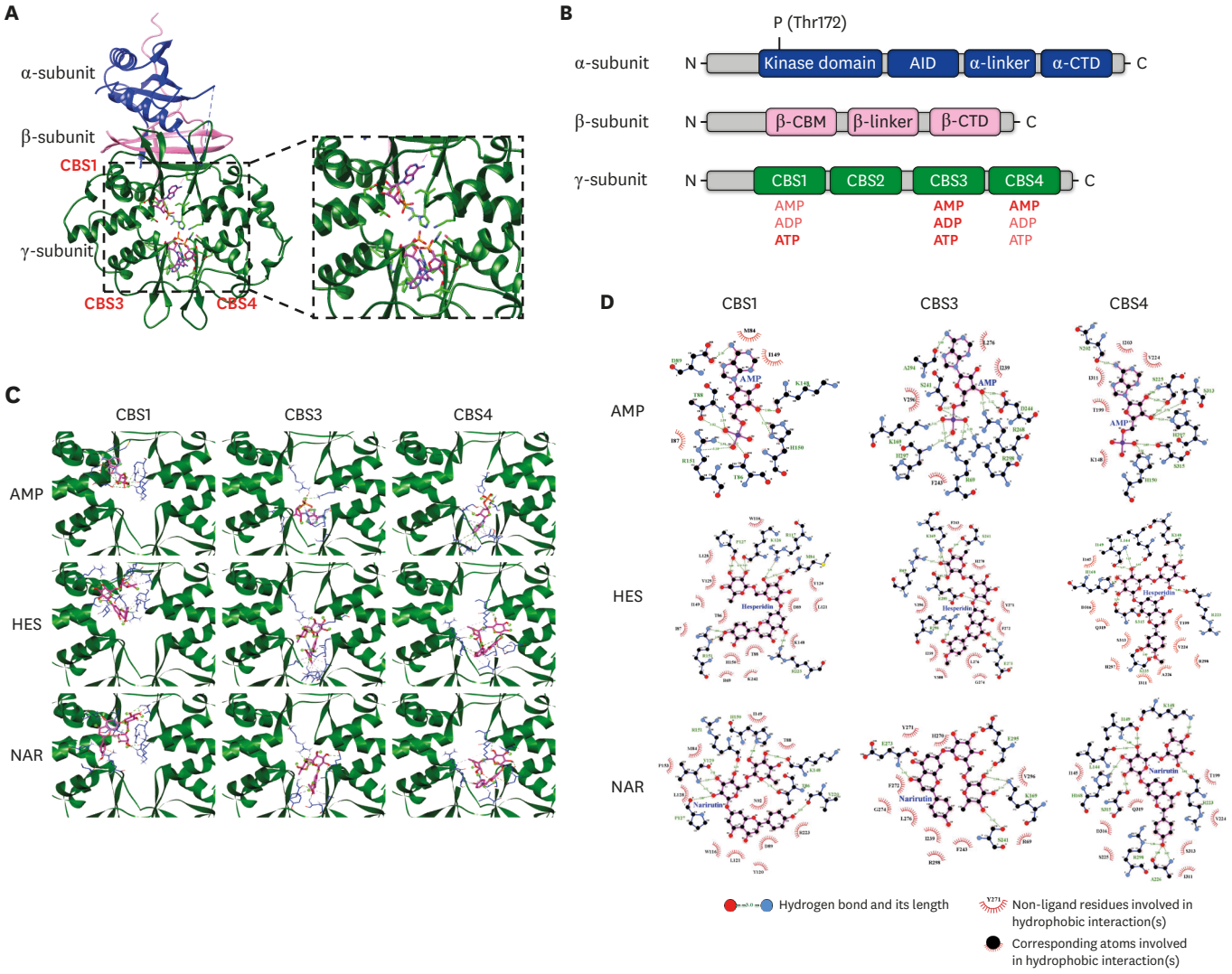

Fig. 7. Molecular docking and the binding interaction of the flavonoids to CBS domains in γ-subunit of AMPK. Heterotrimer of AMPK co-crystallized with three AMP molecules (A). Domain structure of the α, β, and γ subunit of AMPK (B). Interactions of AMP or flavonoids to CBS1, CBS3, and CBS4 domains in the γ-subunit of AMPK (C). Hydrogen bonds and hydrophobic interactions between the flavonoids and γ-subunit of AMPK, which were analyzed using the Ligplot program (D). AMPK, AMP-activated protein kinase; AID, autoinhibitory domain; CBM, carbohydrate-binding module; CTD, C-terminal domain; CBS, cystathionine beta-synthase; HES, hesperidin; NAR, narirutin.

citrus peel flavonoids reduces the intracellular TG content in oleic acid-induced HepG2 cells [12]. In addition, tangeretin can reduce the lipid accumulation and TG content in the liver of high-fat diet-induced obese mice [18]. Hence, flavonoids could play an essential role in reducing intracellular lipid accumulation and the TG content induced by PA in HepG2 cells.

In the present study, the flavonoid treatments increased the AMPK and ACC phosphorylation levels and decreased the SREBP-2 and HMGCR expression levels in PA-treated HepG2 cells. The activation of AMPK is involved in regulating liver lipogenesis, lipid oxidation, and cholesterol synthesis via protein phosphorylation or differential gene expression [19,20]. Moreover, the activation of AMPK enhances the phosphorylation of ACC, which is a crucial rate-limiting enzyme involved in fatty acid biosynthesis [21]. The phosphorylation of ACC leads to its inactivation, which inhibits the formation of malonyl CoA and de novo lipogenesis and stimulates fatty acid oxidation [22]. Nobiletin phosphorylates AMPK and

https://doi.org/10.4142/jvs.21256

inhibits lipogenesis through ACC phosphorylation in high glucose-treated HepG2 cells [23]. Furthermore, AMPK activation inhibits the transcriptional activity of SREBP-2, which functions as a major transcriptional regulator of cholesterol biosynthesis [24]. HMGCR, a rate-limiting enzyme for cholesterol biosynthesis, is a target gene of SREBP-2 [25]. Apigenin, a plant flavonoid, suppressed the TC and TG contents and decreased the SREBP-2 and HMGCR expression levels in palmitic acid-treated HepG2 cells [26]. Therefore, the flavonoids effectively inhibit lipid accumulation in PA-treated HepG2 cells via the AMPK signaling pathway.

The present study observed that citrus flavonoids increase GSK3β phosphorylation in PA-treated HepG2 cells. AMPK phosphorylates and inhibits its downstream substrate, including GSK3β, which improves glucose utilization for glycogenesis [27]. Nobiletin controls glucose homeostasis by eliciting GSK3β phosphorylation via AMPK in PA-treated HepG2 cells [11]. The activation of AMPK by the flavonoids enhances the glucose uptake in an insulin-independent manner in PA-treated HepG2 cells. Previous studies reported that the flavonoids alone could influence glucose uptake in normal HepG2 cells without PA [11,28]. On the other hand, the present work showed that the flavonoids enhanced the decreased glucose uptake by the PA-treatment significantly through the activation of AMPK in HepG2 cells. The phosphorylation of AMPK promotes the membrane translocation of GLUT2 and enhances glucose uptake in an insulin-independent manner in the liver [4]. Overall, the results show that flavonoids regulate the hepatic glucose metabolism by enhancing glucose uptake and glycogenesis via the AMPK signaling pathway.

In the present study, *in silico* molecular docking showed that the flavonoids bind to all the three CBS domains in the γ-subunit of AMPK. AMPK is a heterotrimer consisting of a catalytic α-subunit and 2 regulatory (β and γ) subunits [7]. The γ-subunit contains four tandem repeats of cystathionine-β-synthase (CBS) domains [29]. Among the 4 CBS domains, 3 (CBS1, CBS3, and CBS4) domains are involved in binding adenine nucleotides, including AMP, ADP, and ATP [30]. AMP binding to CBS domains releases the autoinhibitory domain from the catalytic domain in α-subunit [6]. This active conformation allows Thr172 to be phosphorylated by an upstream kinase, including LKB1 and CaMKKβ [7]. In addition, the active form of AMPK prevents the phosphatases from accessing T172 of the catalytic subunit [31]. An *in silico* previous study reported that kaemferide is a promising AMPK activator [8]. Naringenin has shown an anti-adipogenic effect by binding to the AMP binding sites of the γ-subunit as the agonists of AMPK [9]. In the present study, molecular docking analysis showed that the flavonoids activate AMPK directly as positive modulators by interacting with the R groups of the CBS domains in the γ-subunit of AMPK.

In summary, the present study indicated that the flavonoids reduced the lipid accumulation and TG content in PA-treated HepG2 cells by increasing the AMPK and ACC phosphorylation levels while reducing the SREBP-2 and HMGCR expression levels (**Fig. 8**). In addition, the flavonoid-mediated AMPK activation increased the glucose uptake and the phosphorylation of GSK3β, thereby enhancing glycogen synthesis. A future study will examine the expression of genes involved in the esterification of fatty acid in PA-treated HepG2 cells. The overall results suggest that citrus flavonoids have anti-adipogenic effects on PA-treated HepG2 cells via the AMPK signaling pathway. These findings offer a valuable clue for elucidating the mechanism of the anti-adipogenic effect of these flavonoids for the treatment of obesity.

https://doi.org/10.4142/jvs.21256

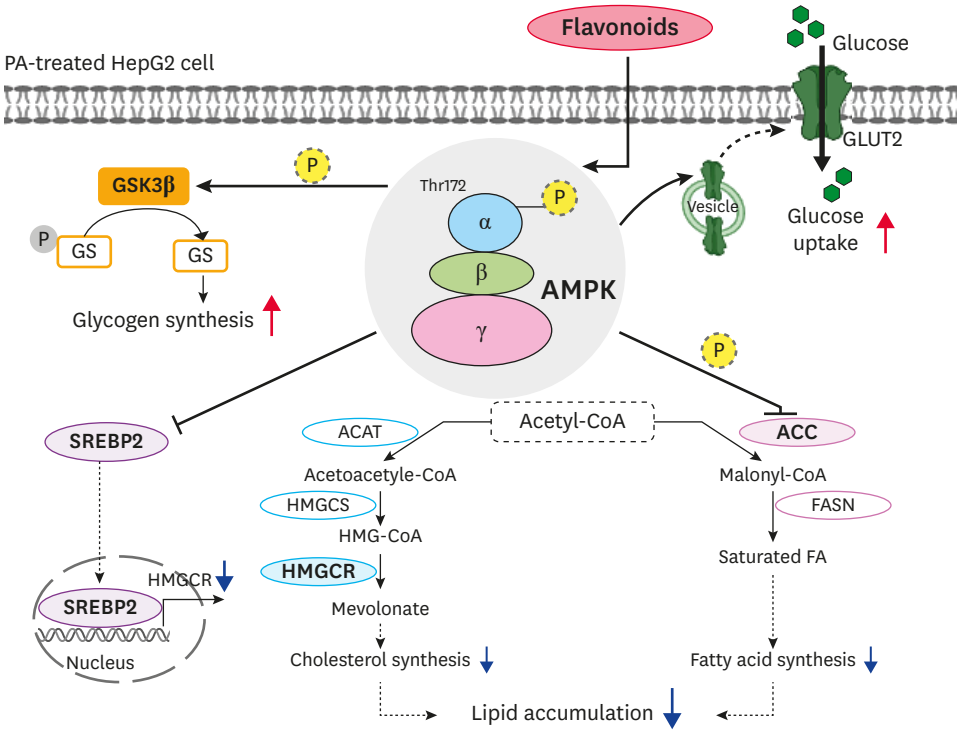

Fig. 8. Proposed mechanism for the anti-adipogenic effect of the flavonoids associated with AMPK activation in PA-treated HepG2 cells.
AMPK, AMP-activated protein kinase; ACC, acetyl-CoA carboxylase; FASN, fatty acid synthase; SREBP-2, sterol regulatory element-binding protein 2; ACAT, acyl-CoA:cholesterol acyltransferase; HMGCS, hydroxymethylglutaryl-CoA synthase; HMGCR, 3-hydroxy-3-methyl-glutaryl-CoA reductase; GLUT2, glucose transporter 2; GSK3β, glycogen synthase kinase 3 beta; GS, glycogen synthase.

REFERENCES

1. Ahmad B, Serpell CJ, Fong IL, Wong EH. Molecular mechanisms of adipogenesis: the anti-adipogenic role of AMP-activated protein kinase. Front Mol Biosci. 2020;7:76.
PUBMED | CROSSREF
2. Jiménez-Sánchez C, Olivares-Vicente M, Rodríguez-Pérez C, Herranz-López M, Lozano-Sánchez J, Segura-Carretero A, et al. AMPK modulatory activity of olive-tree leaves phenolic compounds: bioassay-guided isolation on adipocyte model and in silico approach. PLoS One. 2017;12(3):e0173074.
PUBMED | CROSSREF
3. Wang Q, Liu S, Zhai A, Zhang B, Tian G. AMPK-mediated regulation of lipid metabolism by phosphorylation. Biol Pharm Bull. 2018;41(7):985-993.
PUBMED | CROSSREF
4. Zhu D, Zhang N, Zhou X, Zhang M, Liu Z, Liu X. Cichoric acid regulates the hepatic glucose homeostasis via AMPK pathway and activates the antioxidant response in high glucose-induced hepatocyte injury. RSC Advances. 2017;7(3):1363-1375.
CROSSREF
5. Yuan HD, Kim DY, Quan HY, Kim SJ, Jung MS, Chung SH. Ginsenoside Rg2 induces orphan nuclear receptor SHP gene expression and inactivates GSK3β via AMP-activated protein kinase to inhibit hepatic glucose production in HepG2 cells. Chem Biol Interact. 2012;195(1):35-42.
PUBMED | CROSSREF
6. Xin FJ, Wang J, Zhao RQ, Wang ZX, Wu JW. Coordinated regulation of AMPK activity by multiple elements in the α-subunit. Cell Res. 2013;23(10):1237-1240.
PUBMED | CROSSREF
7. Ross FA, MacKintosh C, Hardie DG. AMP-activated protein kinase: a cellular energy sensor that comes in 12 flavours. FEBS J. 2016;283(16):2987-3001.
PUBMED | CROSSREF

8. Yong Y, Shin SY, Jung Y, Jung H, Ahn S, Chong Y, et al. Flavonoids activating adenosine monophosphate-activated protein kinase. J Korean Soc Appl Biol Chem. 2015;58(1):13-19.
CROSSREF
9. Yang Y, Wu Y, Zou J, Wang YH, Xu MX, Huang W, et al. Naringenin attenuates non-alcoholic fatty liver disease by enhancing energy expenditure and regulating autophagy via AMPK. Front Pharmacol. 2021;12:687095.
PUBMED | CROSSREF
10. Kim DS, Lim SB. Extraction of flavanones from immature *Citrus unshiu* pomace: process optimization and antioxidant evaluation. Sci Rep. 2020;10(1):19950.
PUBMED | CROSSREF
11. Qi G, Guo R, Tian H, Li L, Liu H, Mi Y, et al. Nobiletin protects against insulin resistance and disorders of lipid metabolism by reprogramming of circadian clock in hepatocytes. Biochim Biophys Acta Mol Cell Biol Lipids. 2018;1863(6):549-562.
PUBMED | CROSSREF
12. Su D, Liu H, Qi X, Dong L, Zhang R, Zhang J. Citrus peel flavonoids improve lipid metabolism by inhibiting miR-33 and miR-122 expression in HepG2 cells. Biosci Biotechnol Biochem. 2019;83(9):1747-1755.
PUBMED | CROSSREF
13. Xiong H, Wang J, Ran Q, Lou G, Peng C, Gan Q, et al. Hesperidin: a therapeutic agent for obesity. Drug Des Devel Ther. 2019;13:3855-3866.
PUBMED | CROSSREF
14. Zhao NQ, Li XY, Wang L, Feng ZL, Li XF, Wen YF, et al. Palmitate induces fat accumulation by activating C/EBPβ-mediated G0S2 expression in HepG2 cells. World J Gastroenterol. 2017;23(43):7705-7715.
PUBMED | CROSSREF
15. Malik SA, Acharya JD, Mehendale NK, Kamat SS, Ghaskadbi SS. Pterostilbene reverses palmitic acid mediated insulin resistance in HepG2 cells by reducing oxidative stress and triglyceride accumulation. Free Radic Res. 2019;53(7):815-827.
PUBMED | CROSSREF
16. Liu JY, Zhang YC, Song LN, Zhang L, Yang FY, Zhu XR, et al. Nifuroxazide ameliorates lipid and glucose metabolism in palmitate-induced HepG2 cells. RSC Advances. 2019;9(67):39394-39404.
CROSSREF
17. Kramer B, Rarey M, Lengauer T. Evaluation of the FLEXX incremental construction algorithm for protein-ligand docking. Proteins. 1999;37(2):228-241.
PUBMED | CROSSREF
18. Kim MS, Hur HJ, Kwon DY, Hwang JT. Tangeretin stimulates glucose uptake via regulation of AMPK signaling pathways in C2C12 myotubes and improves glucose tolerance in high-fat diet-induced obese mice. Mol Cell Endocrinol. 2012;358(1):127-134.
PUBMED | CROSSREF
19. Kahn BB, Alquier T, Carling D, Hardie DG. AMP-activated protein kinase: ancient energy gauge provides clues to modern understanding of metabolism. Cell Metab. 2005;1(1):15-25.
PUBMED | CROSSREF
20. Carling D. The AMP-activated protein kinase cascade--a unifying system for energy control. Trends Biochem Sci. 2004;29(1):18-24.
PUBMED | CROSSREF
21. Chen L, Duan Y, Wei H, Ning H, Bi C, Zhao Y, et al. Acetyl-CoA carboxylase (ACC) as a therapeutic target for metabolic syndrome and recent developments in ACC1/2 inhibitors. Expert Opin Investig Drugs. 2019;28(10):917-930.
PUBMED | CROSSREF
22. Foretz M, Viollet B. Activation of AMPK for a break in hepatic lipid accumulation and circulating cholesterol. EBioMedicine. 2018;31:15-16.
PUBMED | CROSSREF
23. Yuk T, Kim Y, Yang J, Sung J, Jeong HS, Lee J. Nobiletin inhibits hepatic lipogenesis via activation of AMP-activated protein kinase. Evid Based Complement Alternat Med. 2018;2018:7420265.
PUBMED | CROSSREF
24. Luo J, Yang H, Song BL. Mechanisms and regulation of cholesterol homeostasis. Nat Rev Mol Cell Biol. 2020;21(4):225-245.
PUBMED | CROSSREF
25. Sakakura Y, Shimano H, Sone H, Takahashi A, Inoue N, Toyoshima H, et al. Sterol regulatory element-binding proteins induce an entire pathway of cholesterol synthesis. Biochem Biophys Res Commun. 2001;286(1):176-183.
PUBMED | CROSSREF

26. Lu J, Meng Z, Cheng B, Liu M, Tao S, Guan S. Apigenin reduces the excessive accumulation of lipids induced by palmitic acid via the AMPK signaling pathway in HepG2 cells. Exp Ther Med. 2019;18(4):2965-2971.
PUBMED | CROSSREF

27. Ha T, Trung TN, Hien TT, Dao TT, Yim N, Ngoc TM, et al. Selected compounds derived from Moutan Cortex stimulated glucose uptake and glycogen synthesis via AMPK activation in human HepG2 cells. J Ethnopharmacol. 2010;131(2):417-424.
PUBMED | CROSSREF

28. Zhang J, Sun C, Yan Y, Chen Q, Luo F, Zhu X, et al. Purification of naringin and neohesperidin from Huyou (*Citrus changshanensis*) fruit and their effects on glucose consumption in human HepG2 cells. Food Chem. 2012;135(3):1471-1478.
PUBMED | CROSSREF

29. Xiao B, Heath R, Saiu P, Leiper FC, Leone P, Jing C, et al. Structural basis for AMP binding to mammalian AMP-activated protein kinase. Nature. 2007;449(7161):496-500.
PUBMED | CROSSREF

30. Carling D, Mayer FV, Sanders MJ, Gamblin SJ. AMP-activated protein kinase: nature's energy sensor. Nat Chem Biol. 2011;7(8):512-518.
PUBMED | CROSSREF

31. Jeon SM. Regulation and function of AMPK in physiology and diseases. Exp Mol Med. 2016;48(7):e245.
PUBMED | CROSSREF